Earthquakes and Structures, *Vol. 12, No. 5 (2017) 479-487*
DOI: https://doi.org/10.12989/eas.2017.12.5.479

The study of frictional damper with various control algorithms

Hamid Rahmani Samani, Masoud Mirtaheri* and Amir Peyman Zandi

Department of Civil Engineering, K.N. Toosi University of Technology, Tehran, Iran

(Received March 14, 2017, Revised April 29, 2017, Accepted May 3, 2017)

Abstract. Frictional dampers are used in structural engineering as means of passive control. Meanwhile, frictional damper shave a disadvantage compared to viscous rivals since the slippage force must be exceeded to activate the device, and cannot be ideal full range of possible events. The concept of semi-active control is utilized to overcome this shortcoming. In this paper, a new semi-active frictional damper called Smart Adjustable Frictional (SAF) damper is introduced. SAF damper consists of hydraulic, electronic units and sensors which are all linked with an active control discipline. SAF acts as a smart damper which can adapt its slippage threshold during a dynamic excitation by measuring and controlling the structural response. The novelty of this damper is, while it controls the response of the structure in real time with acceptable time delay. The paper also reports on the results of a series of experiments which have been performed on SAF dampers to obtain their prescribed hysteretic behavior for various control algorithms. The results show that SAF can produce the desired slippage load of various algorithms in real time. Numerical models incorporating control simulations are also made to obtain the hysteretic response of the system which agrees closely with test results.

Keywords: frictional damper; energy dissipation; passive control; semi-active control; SAF damper

1. Introduction

Frictional dampers are widely used for a seismic design of structures. Since the concept of the structural control utilizing frictional dampers was first proposed by Pall *et al.* (1980). This field has evolved into a practical technology and frictional dampers are widely implemented as an effective approach to control civil engineering structures. To date, many newly developed frictional based energy dissipating devices have been introduced and implemented to enhance the performance of structures (Mualla and Belev 2002, Wua *et al.* 2005, Monir and Zeynali 2013, Mirtaheri *et al.* 2011, Rahmani Samani *et al.* 2014). However, due to their passive nature, conventional frictional dampers cannot alter their mechanical properties in real time in order to best suit the structural responses. In other words, the concept of semi-active control has not been utilized to improve the efficiency of frictional dampers. Semi-active control technology is now receiving considerable attention from mechanical and civil engineering professionals. This is due to the fact that it offers the reliability of passive control and at the same time maintains the versatility and adaptability of active control with a much lower power requirement. Furthermore, stability of a semi-active system is not compromised by any controller i.e. the forces generated by a semi-active frictional damper are always dissipative in nature. A semi-active frictional damper adapts its slippage threshold during earthquake excitation according to structural responses in a smart fashion. Kannan *et al.* (1995) were the pioneers by introducing Active Slip Bracing Device (ASBD). The device allows the brace to axially elongate or contract through slippage when the brace loads reach the slippage force, which is controlled by a hydraulic actuator. Its main disadvantage is that it cannot rapidly modulate the actuation force for the contacting force to reach the required pressure and it may introduce the backlash effect when used. Agrawal and Yang (2000) proposed an electromagnetic frictional damper. This device is based on the regulation of friction force across the damper using electromagnetic field. However, activating force of electromagnetic based devices can produce forces which are rather small in value which is not sufficient to produce the required forces. Gaul *et al.* (2004) proposed semi-active joint connections in which piezoelectric stack disc is utilized as a washer to control in real time the normal force induced in the friction interface of joints, based on the feedbacks from a sensor. If a voltage is applied to the piezoelectric washer, the stack disc tends to expand, which results in increasing the normal force and slippage threshold. Chen and Chen (2000) introduced Piezoelectric Friction Damper (PFD). The clamping force in such a damper is regulated by piezoelectric actuators. However, piezoelectric based frictional dampers are not applied to building structures due to the fact that the forces produced by piezoelectric actuators are rather small in value. Moreover, piezoelectric actuators are not cost effective since high-force piezoelectric actuators are expensive. Samani et al. proposed a novel Adjustable Frictional Damper (AFD) (Rahmani Samani *et al.* 2015). The mechanism of AFD is similar to a car braking system. Samani *et al.* (2016) proposed a new displacement design procedure for frictional damping based structural system. By utilizing the system, the slip loads of the dampers are

* Corresponding author, Associate Professor
E-mail: mmirtaheri@kntu.ac.ir

http://www.techno-press.com/journals/eas&subpage=7 ISSN: 2092-7614 (Print), 2092-7622 (Online)

chosen such that target displacement is satisfied.

The performance of passive control system for the seismic protection of a multi-tower cable-stayed bridge with the application of partially longitudinal constraint system was investigated by Fang *et al*. (2014). Casciati and Domaneschi (2007) presented the characterization of an electro-inductive device with semi-active behavior in detail. The paper also discusses ways of building a semi-active device, and details its passive control function.

A passive structural control system was studied through nonlinear numerical analyses carried out in time domain for several seismic realizations in a multiple support framework (Domaneschi and Martinelli 2012). Domaneschi and Martinelli (2014) proposed updated bridge model. Murase *et al*. (2013) studied Smart passive control of buildings with higher redundancy and robustness using base-isolation and inter-connection. Domaneschi (2012) deals with a method of controlling in real time the hysteresis component in simulated semi-active control systems through the Bouc-Wen model. An introductive discussion on the theoretical formulation of the original settlement allows focusing on a way for tuning the parameters which can be managed for hysteresis regulation. Proper algorithms, embedded into the analytical formulation of the model, are subsequently selected for implementing the semi-active characteristic. Finally, straightforward dynamic applications on a plane oscillator system point out the general capability of the proposed approach by seismic response simulation and mitigation of the induced structural effects.

Introduced in this paper, is a semi-active frictional damper called Smart Adjustable Frictional (SAF) damper. SAF dampers are multifunctional devices, which not only can be used as semi-active frictional dampers but also can emulate semi-active viscous dampers. In order to show the effectiveness of SAF dampers, a series of experiments have been performed utilizing various algorithms to obtain its hysteretic behavior. Numerical models which incorporate both finite element and control simulations are also developed. In this paper the main components of SAF dampers and the prototype manufactured by this concept are introduced. Then, various control algorithms for semi-active frictional dampers are explained, followed by the dynamic cyclic tests in order to obtain the hysteretic behavior of the prototypes. Finally, numerical simulations of the system are presented. The device introduced in this paper is only to demonstrate the feasibility of construction of an integrated system of mechanical, electrical and hydraulic devices for implementation as regard to frictional damper. This system is only a prototype in a laboratory scale capable of producing relatively small forces. Of course for a real structural system a much more robust mechanism is required. Current research is under way to show such system. This system requires very little maintenances since it is made of stainless steel and will easily be powered by a UPS emergency system.

2. Components and mechanism of SAF dampers

SAF dampers consist of mechanical and hydraulic systems which are incorporated by an electronic sensor system all linked together in a multi-disciplinary fashion. Mechanical and hydraulic units provide forces in order to produce clamping pressures, which in turn creates frictional resistance. Electronic unit acts as a command and control system. Sensors provide the necessary feedback of acceleration and displacements to the system. All of these components are described fully in following sections.

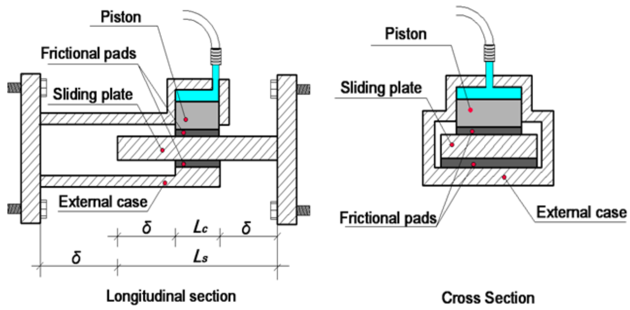

(a) (b)

Fig. 1 Typical configuration of SAF damper; a. longitudinal section; b. Cross section

2.1 Mechanical unit

The mechanical unit of SAF damper is very similar to a vehicle braking system. This unit consists of three main parts; external case, piston and sliding plate. Fig. 1 shows the typical configuration of SAF damper. As shown in this figure, the clamping force is provided by the hydraulic pressure exerted on the piston. Since SAF dampers are very similar to an automobile disk braking system the prototype is based on an actual braking system of a typical automobile. Fig. 2 shows the prototype of the mechanical unit. The external case is made of cast iron and the connection plates are made of structural mild steel conforming to ASTM A36. Plating is used as finishing of the connection plates and corrosion resistance. The sliding plate is made out of stainless steel (A36). All the plates are machined to the exact dimensions determined by designed parameters. The diameter of the piston is 48 mm. Dimensions of the sliding plate is 55 mm in width and 4 mm in thickness. The frictional pads are made of a semi-metallic material with ability to resist brake fade at

(a) (b)

Fig. 2 Typical configuration of SAF damper; a. longitudinal section; b. Cross section increased temperatures. Pads are approximately rectangular dimensioning 80×40×14 mm. The coefficients of static and dynamic frictions (μ_s, μ_k) are obtained based on several tests giving 0.12 for μ_s and 0.1 for μ_k.

2.2 Hydraulic unit

The hydraulic unit is composed of an oil reservoir, a pump, an electromotor which provides pressure and a pressure control proportional solenoid valve. The valve pressure can be modulated continuously in proportion to the electrical current supplied to the solenoid. The valve can be controlled directly by a current control supply unit or by means of the relative electronic control unit to optimize valve performance. The step response of the valve is defined as the time taken for the valve to reach 90% of the set pressure value. This time is measured to be 80 milliseconds.

2.3 Electronic unit

Electronic unit is the controller of the system. The core of this unit is a Programmable Logic Controller (PLC) and a Human Machine Interface (HMI). The PLC read the input signal from the sensors called neurons of the system. Then the input signals are processed according to the selected algorithm, and subsequently the output signal is sent to the proportional valve. The HMI enables the user to select the desired control algorithm and set some variables which are described later in this paper. Also, HMI reports the status of the dampers in terms of relative displacement and input signal the control algorithms are described in section 3. Fig. 3 shows the electronic and hydraulic units linked together.

2.4 Sensory system

The sensory system is composed of the Linear Variable Displacement Transducers (LVDTs) and accelerometers. The fabricated prototype is equipped with one LVDT and a three directional accelerometer.

If the acceleration which is sensed by the accelerometer exceeds a_0 m/s^2 the PLC starts the pump and if the acceleration became less than a_0 m/s^2 for more than t_{off} seconds the PLC automatically turn off the pump, which in turns cut off the hydraulic pressure. Both a_0 and t_{off} may be set by the user through HMI. The default values of a_0 and t_{off} are 0.1 m/s^2 and 10 seconds respectively.

Fig. 3 Electronic and hydraulic units linked together

3. Control algorithms

The performance of the structure equipped with SAF dampers significantly relies on the applied control algorithm. The algorithm determines how to adjust the slippage load so that the desired dynamic characteristics are achieved. Various control strategies are already developed for semi-active frictional dampers. Dowdell and Cherry (1994) are among the researchers who investigated the dynamic response of the structural systems equipped with semi-active frictional dampers. They developed on-off control method. This method utilizes simple algorithms that require only the feedback of inter-story velocity of the story in which a semi-active damper such as SAF is located. The slippage force of the i-th damper, F_{si}, is given by

$$F_{si} = \begin{cases} F_{so} & |v_i| > 0 \\ 0 & |v_i| = 0 \end{cases} \tag{1}$$

Where v_i is the i-th inter-story velocity. At the moment when a reversal of the direction in the inter-story drift is detected, the slippage load is momentarily reduced from its predetermined value, F_{so}, to near zero. When the slippage force is released (off state), the brace slips to a new position which in turns increase the clamping force in the friction surface to its predetermined value (on state). Utilizing on-off algorithm the friction damper is always at the threshold of the slippage state even for low level external excitations. The repetitive damper actions in 'on' and 'off' states which is similar to anti-locking brake system in automobile, result in a discontinuous control force that can exert a high-frequency structural response and amplify structural acceleration.

Akbay and Aktan proposed a simple control algorithm namely incremental frictional force control that determines the next time-step clamping force by one pre-specified increment of the current force at a fixed time step (Akbay Aktan 1995). At each sampling interval a decision on the clamping force is made. If the device is in motion along the friction surface, then the slippage load is increased one increment; otherwise, the slippage load is decreased one increment. Therefore, the control algorithm proposed is similar to on-off algorithm; since both make decisions according to the inter-story velocity. The latter algorithm, somewhat reduces the problem of high speed switching. However, it may also cause discontinuous control forces. Furthermore; in order to obtain a better performance, the algorithm requires the proper determination of the increment of the clamping force and the control time interval.

Inaudi (1997) proposed a control strategy called Modulated Homogenous Friction (MHF) that produces a slip force proportional to the prior local peak of the damper deformation. Mathematically, the controller is expressed as

$$F_s(t) = \mu g \left| P[\Delta(t)] \right| \tag{2}$$

Where g is the positive gain coefficient with units of stiffness, μ is friction coefficient and $P[\Delta(t)]$ the operator defined as follows

$$P[\Delta(t)] = \Delta(t-s) \qquad s = \left\{ \min x \geq 0 : \frac{d\Delta}{dt}(t-x) = 0 \right\} \tag{3}$$

Where $\Delta(t\text{-}s)$ is a local peak of the deformation signal. The absolute value of $\left| P[\Delta(t)] \right|$ is due to the required positive slippage forces. Since the output of $P[\Delta(t)]$ is equal to the value of the input signal at the prior closest local peak $P[\Delta(t)]$ is referred to as prior-local-peak operator. More information regarding the parameters of Eq. (3) is provided in this study. The algorithm may also cause discontinuous control forces and the device may not be operational in all moments. It is important for the controller to maintain the SAF damper in the sliding mode as long as possible to maximize the dissipation of energy. He *et al.* (2003) modified the MHF strategy in order the damper to be continually operational during excitation. The mathematical expression may be given by

$$F_s(t) = \mu g \left| P[\Delta(t)] \right| \tanh(\alpha v) \tag{4}$$

Where v is inter-story velocity and α is a parameter representing the measure of the thickness of the boundary layer in the vicinity of v=0. This algorithm is called, Smooth Boundary Layer Semi-Active Friction (SBLSAF) controller.

It should be mentioned that although the failure of electricity networks is a common occurrence in major earthquakes, this shortcoming can be rectified by utilization of systems like UPS (Uninterruptible power supply).

4. Experimental study of hysteretic behavior of the SAF

Uniaxial tests are performed to determine the axial force-displacement relationship of the SAF damper. The tests are conducted at displacement levels which are below the lockout value of the damper.

4.1 Test setup

SAF damper specimen is tested in a universal testing machine in vertical position as shown in Fig. 4. The testing machine had a capacity of 250 kN and 500 mm of travelling range. Force and displacement were measured by internal load cell and LVDT and recorded by a data acquisition system. Hysteretic force-displacement curves are determined through this data.

4.2 Full cycle loading

Various constant voltages and consequently constant pressures are applied to the prototype SAF damper to observe its characteristics. Typical force displacement

Fig. 4 SAF damper specimen in universal testing machine

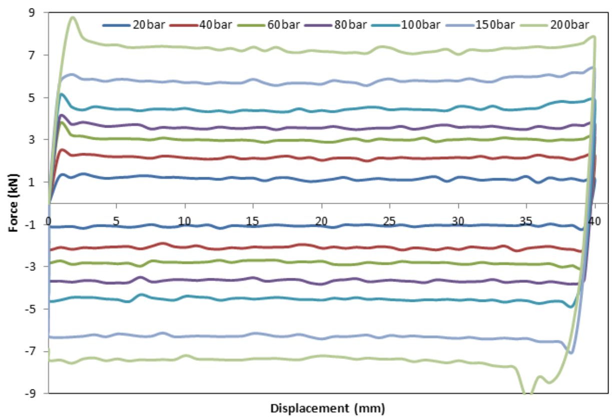

Fig. 5 Slippage load of SAF damper for various pressures

curves obtained for amplitude of 40 mm is shown for constant clamping pressures of 20 bars, 40 bars, 60 bars, 80 bars, 100 bars, 150 bars and 200 bars are provided in Fig. 5. The figure shows the behavior of system in both compression and tension. As anticipated for higher clamping pressures, higher slippage loads will be obtained.

4.3 Dynamic loading

The test cycles and rates, at which cyclic tests are performed, are shown in Table 1. After each test the specimen is cooled down before performing the next test in order to avoid thermal accumulation.

4.3.1 Anti-locking control algorithm

The Anti-Locking control algorithm is similar to on-off strategy described in section 3. The slippage force of the SAF is expressed as

$$F_s = \begin{cases} F_{s0} & |v| > v_0 \\ 0 & |v| = v_0 \end{cases} \tag{5}$$

Where F_s is the slippage threshold of the damper, v is the

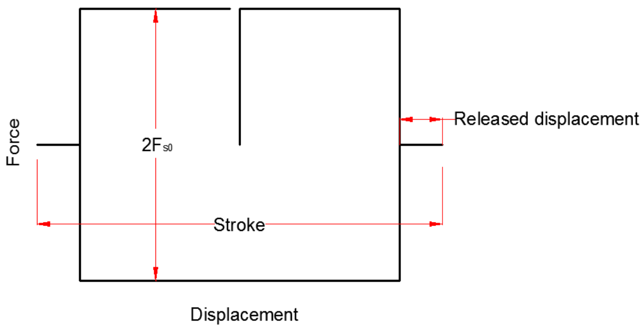

Fig. 6 Typical hysteretic curve of the anti-locking algorithm

relative velocity between the sliding plate and friction pads. A typical hysteretic curve of the anti-locking algorithm is shown in Fig. 6.

The length of the released displacement is related to the parameter v_0. The lower results in less released displacement. For v_0=0 the hysteretic curve become similar to hysteretic curve for passive frictional dampers. Fig. 7 shows the theoretical hysteretic curve of anti-locking algorithm under a sinusoidal function $d(t)$=0.2 sin(πt) as the harmonic excitation. The values of F_{s0} and are assumed to be 3 kN and 0.02 m/s respectively. These values correspond to the values used for tests. However, the data sampling rate can affect the general hysteresis behavior which is reflected on various curves. Figs. 7(a) and 7(b) represent the theoretical hysteresis curves for data sampling period of 0.01 sec and 0.05 sec respectively. Another parameter that can affect the hysteresis behavior is time delay of the system, t_d. Due to operation of proportional valve. Fig. 7(c) shows the theoretical hysteretic curve of anti-locking algorithm assuming 0.05 sec time delay and data sampling rate of 0.05 sec. The experimental hysteretic curves found from tests with this control algorithm for F_{s0}=3 kN and $v_0 = 0.02\frac{m}{s}$ are shown in Fig. 8 which closely agrees with theoretical curve of Fig. 7(c), regarding the sampling rate and time delay. Although this frictional smart damper is tested under forces around 3 kN and which seems low, the purpose of this test was to demonstrate the multi-disciplinary technology which can be expanded and utilized in real structures.

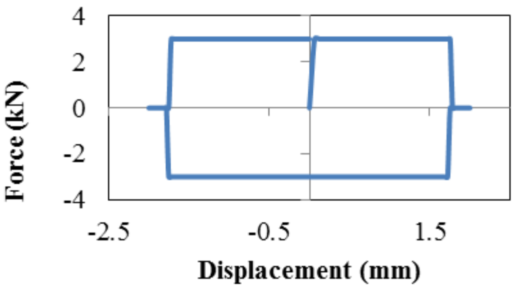

(a)

Fig. 7 Effect of time delay on hysteretic behavior of anti-locking algorithm

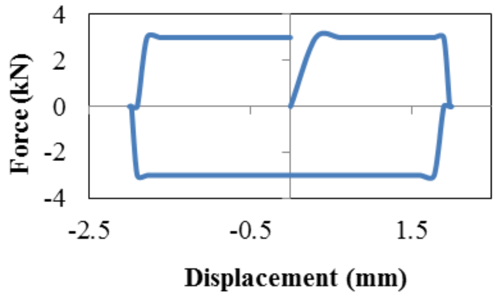

(b)

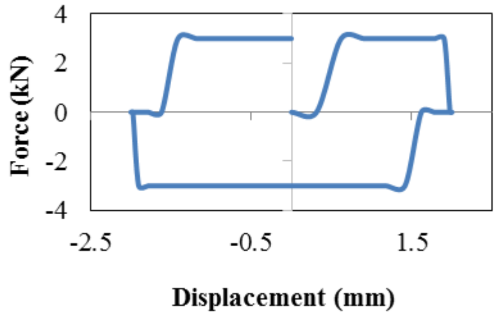

(c)

Fig. 7 Continued

4.3.2 Modulated homogenous friction

As explained in section 3, Modulated Homogenous Friction (MHF) produces a slippage force proportional to the prior local peak of the damper deformation. This algorithm is introduced to SAF damper as follows

$$P(t) = k\left|P[\Delta(t)]\right| \tag{6}$$

Where P is the hydraulic pressure and $P[\Delta(t)]$ is prior-local-peak operator. k is selected to be 2 bar/mm. A sinusoidal displacement with increasing amplitude is imposed to the device. The displacement recorded by the LVDT is shown in Fig. 9. A graphical comparison of the desired pressure and the theoretical pressure is shown on Fig. 10(a) and (b) shows the normalized recorded pressure and imposed displacement. Finally, Fig. 11 represents the experimental hysteretic curves of the above algorithm. As it can be seen from this figure the slippage load adjusts itself according to applied displacement in a smart and controlled fashion.

4.3.3 Velocity proportional (viscous) algorithm

SAF damper is a multifunctional device which not only can be used as a semi-active frictional damper but can also emulate viscous dampers. In order to work as the viscous damper, the slippage load of the damper is defined as follows in control algorithm

$$P(t) = cv \tag{7}$$

Where v is the relative velocity between the sliding plate and frictional pads and c is the damping constant. Fig. 12(a) shows the experimental hysteretic curve of this algorithm for damping constant of $c = 1\dfrac{bar.\sec}{mm}$. A sinusoidal function $d(t)$=0.2 sin(πt) is used as the harmonic excitation. Fig. 12(b) shows the time-histories of the required pressure as well as recorded pressure during the test period. The proportional valve can provide the necessary pressure with acceptable time delay and accuracy.

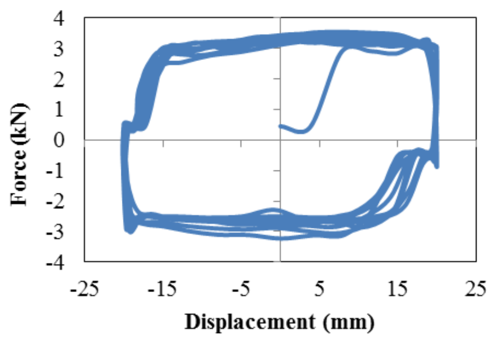

Fig. 8 Experimental hysteretic curve for case A

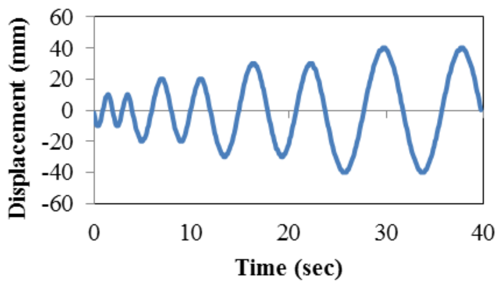

Fig. 9 Time history of the imposed displacement for experimental test of MHF

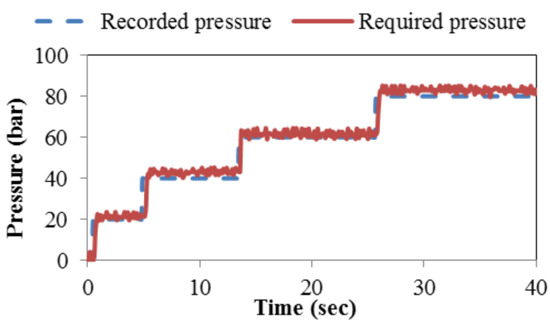

(a)

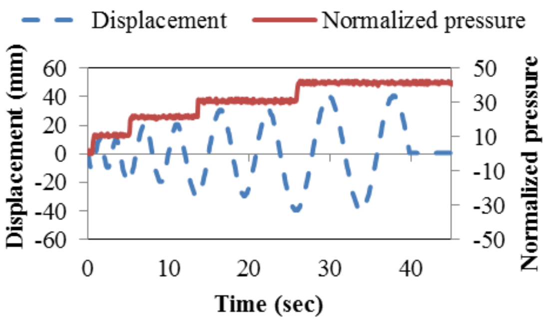

(b)

Fig. 10 (a) Comparison of recoded and theoretical pressure; (b) Time histories of pressure and displacement

4.3.4 Semi-passive control

Most of passive frictional dampers are made of a set of steel plates with certain friction coefficient that are forced by bolt pretention in order to induce the friction between the involved elements. Using pre-tensioned bolts for inducing friction, makes the behavior of frictional dampers unpredictable. The relaxation or loosening of the clamping elements contributes to this unpredictably and may lead to decay of slippage load. SAF dampers may also be utilized as a passive damper as long as the hydraulic pressure and thus the friction, is kept at a constant value. In this case the slippage load of SAF damper can be conveniently evaluated by measuring the hydraulic pressure and compensated if required. Another important advantage of SAF damper as a semi-passive frictional damper is that re-centering of the system after a severe shock is no longer a concern since the clamping forces may be released temporarily in order to let the inherent stiffness or outer force re-center the system.

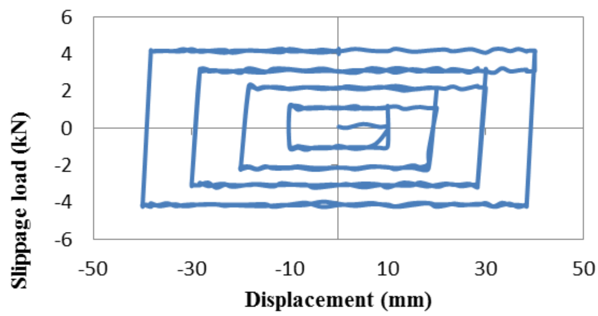

Fig. 11 Experimental hysteretic curve for case B

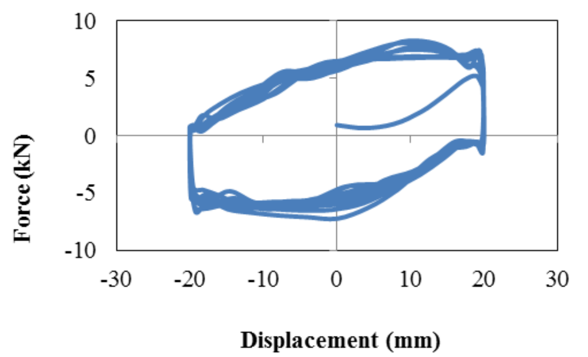

(a)

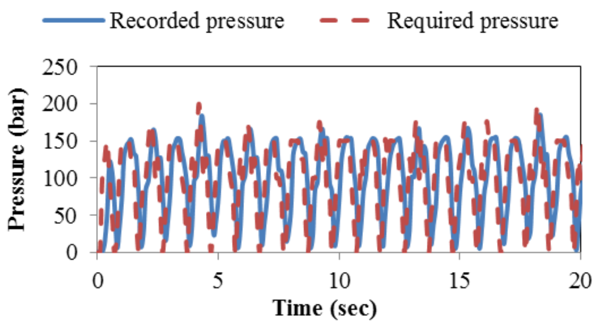

(b)

Fig. 12 (a) Experimental hysteretic curve for viscous algorithm; (b) Comparison of recoded and theoretical pressure

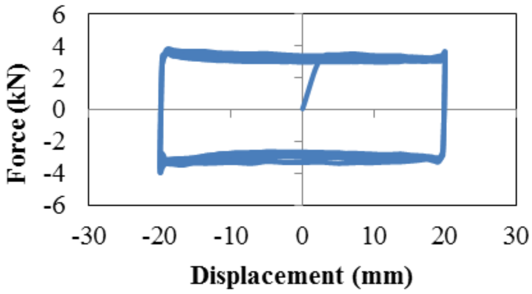

Fig. 13 Experimental hysteretic curve for case D

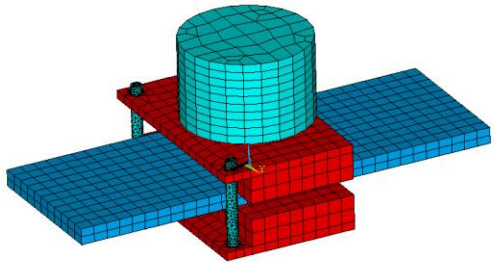

Fig. 14 Finite element model of SAF damper

The hysteretic axial force-displacement curve for passive case is shown in Fig. 13. As one could expect, the SAF damper exhibits classical rectangular hysteresis loops of a passive frictional damper. Furthermore, the SAF damper has almost the same performance in compression and tension.

Although the devices can be utilized as reliable passive similarly fabricated dampers with a wide range of operational capacities, their pressure can be easily changed such that with minimum time delay the system is converted to a semi-active system. Intensive cyclic tests are performed by the Samani *et al*. to achieve the hysteretic behavior of the device in passive mode under various frequencies and it is shown that the hysteretic behavior of the device is not frequency dependent (Rahmani Samani *et al*. 2015).

5. Numerical study of the SAF damper

According to various specifications such as ASCE/SEI 41-06 any type and size of the dampers used in the design must be tested through construction of prototypes before utilizing them in a real structure (ASCE 2006). Such prototypes must be tested with twenty fully reversed cycles at a frequency equal to the fundamental frequency of the structure. Despite the difficulties of tests required by ASCE/SEI 41-06, such tests must be conducted due to the potential unwarranted assumptions and simplifications of numerical models. However, numerical models should be used as a guideline to design the suitable damper.

Three dimensional finite element model of the prototype device is developed as shown in Fig. 14. 20-node brick solid elements are used to model the sliding plate and the frictional pads as well as the piston. These elements have twenty nodes. Surface to surface contact is utilized to simulate the friction between the piston and the upper pad and also between the sliding plate and pads. The modules of elasticity and Poisson's ratio of the sliding plate are taken as 2.1e5 MPa and 0.3 respectively. The boundary condition of the FE model is such that it represents the physical conditions in the actual mechanical setup. The modified newton raphson method is utilised as a solver. Cyclic displacements similar to experiments are applied to the model. As the first step of the analysis, relevant value of hydraulic pressure is applied to the piston according to the selected strategy. Secondly, a displacement history similar to the one used in the experimental test is applied to the model. Fig. 15 shows the flowchart of the numerical analysis. The resulting hysteretic curves are obtained for each algorithm. For comparison between experimental and numerical results the hysteretic curves are superimposed on the same graph in Figs. 16-17. As it can be seen in Fig. 16(a), the numerical results closely match those obtained from experiments. However, in the Fig. 17(a), there is a slight discrepancy between the experimental and numerical results on the first cycles of testing. This is perhaps due to precession of measurement instruments.

6. The effects of heat and wear induced by dynamic loading on hysteretic behavior of SAF damper

During an earthquake excitation, a damper may experience many cycles of dynamic loading. In most kind of dampers such as viscous fluid dampers, visco-elastic dampers, buckling-restrained braces and magneto-rheological (MR), the mechanical energy is converted to heat. Thus energy dissipation is often associated with undesirable self-heating. The effects of heat induced by the cyclic loading subsequently reduce the energy absorption of the damper especially for viscous fluid dampers and MR dampers which are sensitive to temperature change (Makris *et al*. 1998, Gordaninejad and Breese 1999). The effects of heat induced by the cyclic loading on frictional dampers are fully evaluated by Rahmani Samani *et al*. (2014) through numerical models which accounts for thermal-structural interaction and also experiments. The results demonstrate that the slippage load is reduced gradually when subjected to consecutive cycles. This drift is attributed to thermal deformation. However, for SAF damper, the thermal effects are not concerned since the shape of the sliding plate is in such a way that will dissipate the heat rapidly and during all actual tests the maximum recorded temperature was not more than 50°C. Furthermore; the drop of clamping force is immediately compensated.

7. Conclusions

A new semi-active frictional damper called Smart Adjustable Frictional (SAF) damper is introduced in this paper. What is novel about this system as compared to similar existing systems is the fact that the SAF can provide large enough forces in a robust fashion for real time control

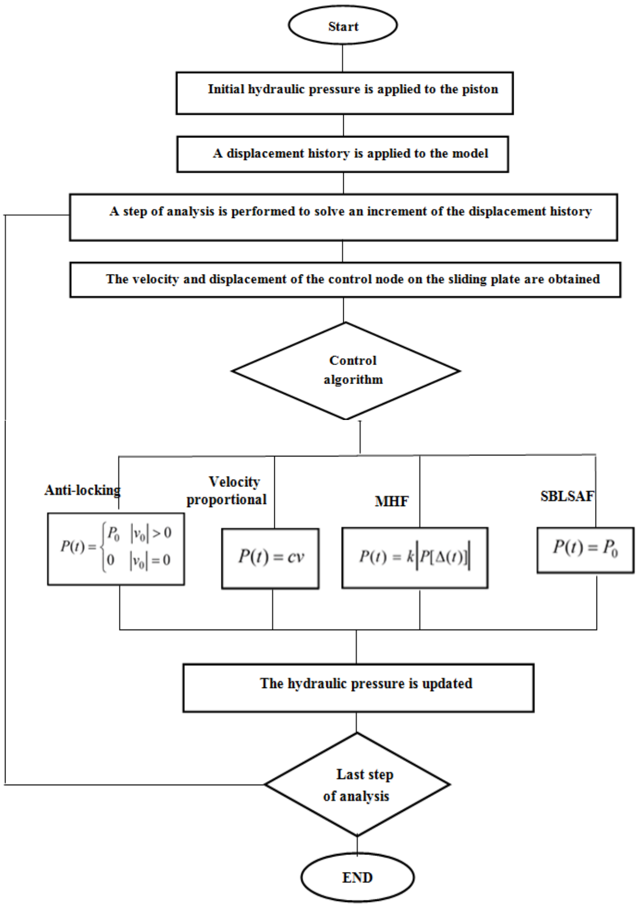

Fig. 15 Flow chart of numerical analysis

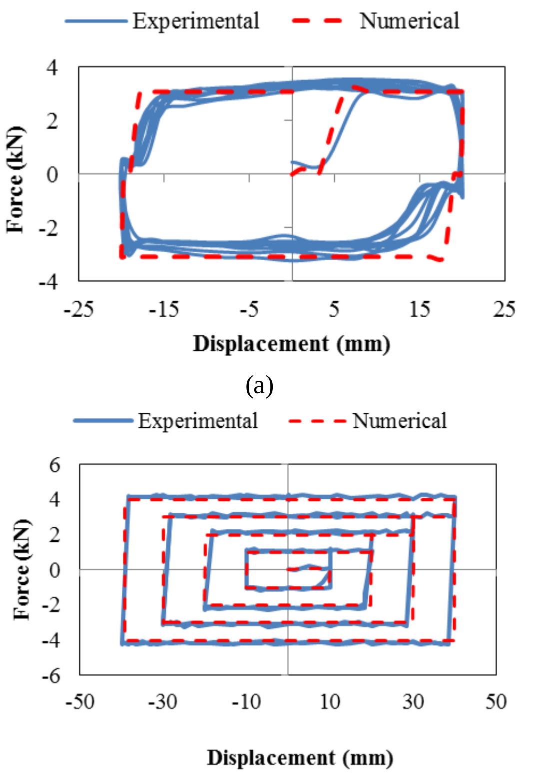

Fig. 16 Comparison of numerical and experimental hys teretic curve for cases: (a) Case A; (b) Case B

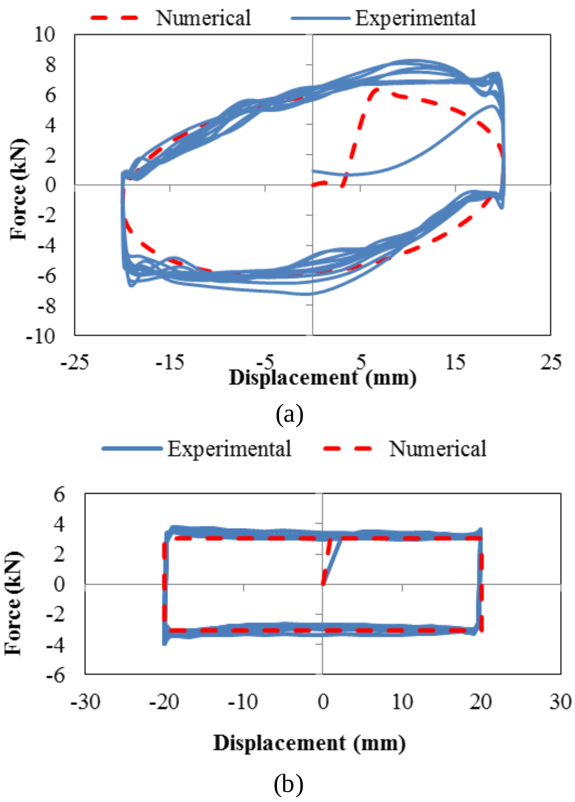

Fig. 17 Comparison of numerical and experimental hysteretic curve for cases; (a) Case C; (b) Case D

of civil and mechanical systems. SAF is not only robust but also it is economical. Series of experiments are performed in order to obtain the hysteretic behavior of SAF dampers utilizing various control algorithms. The results show that SAF damper is able to produce large slippage loads in acceptable time delay. It is also shown that SAF performance is reliable base on comparison between experimental and numerical results, and it is capable to produce the desired slippage load of various algorithms such as on-off and modulated homogenous friction controller. Furthermore, the results show that SAF damper is a multifunctional device which not only can be used as a semi-active frictional damper but also can emulate semi-active viscous dampers. SAF is equipped with a Human Machine Interface (HMI) which enables the user to select the desired control algorithm and also reports the status of the dampers and input signal which can be utilized for health monitoring of the structures.

References

Agrawal, A. and Yang, J. (2000), “A semi-active electromagnetic friction damper for response control of structures”, *ASCE Proceedings of the 2000 Structures Congress and Exposition*, Philadelphia, PA, USA, July.

Akbay, Z. and Aktan, H.M. (1995), “Abating earthquake effects on buildings by active slip brace devices”, *Shock Vib.*, **2**(2), 133-142.

ASCE/SEI 41-06(2006), Seismic rehabilitation of existing buildings. Reston (VA): American Society of Civil Engineers

(ASCE), Reston, VA, USA.

Chen, G.D. and Chen, C.C. (2000), "Behavior of piezoelectric friction dampers under dynamic loading", *Proceedings of SPIE -The International Society for Optical Engineering (Proceedings of SPIE)*, Newport Beach, USA.

Casciati, F. and Domaneschi, M. (2007), "Semi-active electro-inductive devices: Characterization and modelling", *J. Vib. Control*, **13**(6), 815-838.

Domaneschi, M. and Martinelli, L. (2012), "Performance comparison of passive control schemes for the numerically improved ASCE cable-stayed bridge model", *Earthq. Struct.*, **3**(2), 181-201.

Domaneschi, M. and Martinelli, L. (2014), "Extending the benchmark cable-stayed bridge for transverse response under seismic loading", *J. Bridge Eng.*, ASCE, **19**(3), 04013003.

Domaneschi, M. (2012), "Simulation of controlled hysteresis by the semi-active Bouc-Wen Model", *Comput. Struct.*, **106-107**, 245-257

Dowdell, D.J. and Cherry, S. (1994), "Semi-active friction dampers for seismic response control of structures", *Proceeding 5th US national conference on Earthquake Engineering*, Chicago, USA.

Fangfang, G., Youliang, D., Jianyong, S., Wanheng, L. and Aiqun, L. (2014), "Passive control system for seismic protection of a multi-tower cable-stayed bridge", *Earthq. Struct.*, **6**(5), 495-514.

Gaul, L., Albrecht, H. and Wirnitzer, J. (2004), "Semi-active friction damping of large space truss structures", *Shock Vib.*, **11**(3), 73-86.

Gordaninejad, F. and Breese, D.G. (1999), "Heating of magneto rheological fluid dampers", *J. Intel. Mater. Syst. Struct.*, **10**(6), 34-45.

He, W.L., Agrawal, A.K. and Yang, J.N. (2003), "Novel semi-active friction controller for linear structures against earthquakes", *J. Struct. Eng.*, **129**(7), 41-50.

Inaudi, J.A. (1997), "Modulated homogeneous friction: a semi-active damping strategy", *Earthq. Eng. Struct. Dyn.*, **26**(3), 61-76.

Kannan, S., Uras, H.M. and Aktan, H.M. (1995), "Active control of building seismic response by energy dissipation", *Earthq. Eng. Struct.*, **24**(5), 747-759.

Makris, N., Roussos, Y., Whittaker, A.S. and Kelly, J.M. (1998), "Viscous heating of fluid dampers. II: Large-amplitude motions", *J. Eng. Mech.*, ASCE, **124**(11), 17-23.

Mirtaheri, M., Zandi, A.P., Samadi, S.S. and Rahmani Samani, H. (2011), "Numerical and experimental study of hysteretic behaviour of cylindrical friction dampers", *Eng. Struct.*, **33**(12), 47-56.

Monir, H.S. and Zeynali, K. (2013), "A modified friction damper for diagonal bracing of structures", *J. Constr. Steel Res.*, **87**, 17-30.

Mualla, I.H. and Belev, B. (2002), "Performance of steel frames with a new friction damper device under earthquake excitation", *Eng. Struct.*, **24**(3), 65-71.

Murase, M., Tsuji, M. and Takewaki, I. (2013), "Smart passive control of buildings with higher redundancy and robustness using base-isolation and inter-connection", *Earthq. Struct.*, **4**(6), 649-670.

Pall, A.S., Marsh, C. and Fazio, P. (1980), "Friction joints for seismic control of large panel structures", *J. Prestress. Concrete Inst.*, **25**(6), 38-61.

Rahmani Samani, H., Mirtaheri, M., Zandi, A.P. and Bahai, H. (2014), "The effects of dynamic loading on hysteretic behavior of frictional dampers", *Shock Vib.*, **2014**, 1-9.

Rahmani Samani, H., Mirtaheri. M. and Zandi, A.P. (2015), "Experimental and numerical study of a new adjustable frictional damper", *J. Constr. Steel Res.*, **112**, 354-362.

Rahmani Samani, H., Mirtaheri, M. and Hariri-Ardebili, M.A. (2016), "A frictional damping based design methodology for structures", *Struct. Building*, **169**(3), 174-183.

Rahmani Samani, H., Mirtaheri, M. and Rafiei, M. (2015), "The effects of various slippage loads on the response modification factor of steel structures equipped with frictional dampers", *Int. J. Struct. Stab. D.*, **15**(6), 1450080.

Wua, B., Zhanga, J., Williams, B.M.S. and Oua, J. (2005), "Hysteretic behaviour of improved Pall-typed frictional dampers", *Eng. Struct.*, **27**(8), 1258-1267.

CC